

Photocatalytic Production of Hydrogen by Disproportionation of One-Electron-Reduced Rhodium and Iridium–Ruthenium Complexes in Water**

Shunichi Fukuzumi,* Takeshi Kobayashi, and Tomoyoshi Suenobu

Photocatalytic production of hydrogen (H_2) has attracted increasing attention, because H_2 is a clean energy source for the future to reduce dependence on fossil fuels and emissions of greenhouse gases in the long term.^[1,2] Extensive efforts have explored the development of photocatalytic H_2 evolution systems, which consist of an electron donor, a photosensitizer, an electron mediator such as methyl viologen (MV^{2+}), and a hydrogen-evolution catalyst.^[3–15] Both heterogeneous catalysts such as platinum nanoclusters and molecular homogeneous catalysts have been used for the photocatalytic hydrogen evolution.^[3–14] Organorhodium complexes were found to be useful in place of colloidal platinum for TiO_2 photosensitized hydrogen evolution.^[15] However, the detailed photocatalytic mechanism of one-electron transfer among components has yet to be elucidated, because the two-electron reduction of protons is required for H_2 production. In particular, it should be clarified how photoinduced electron transfer of a photosensitizer (a one-electron process) leads to H_2 production (a two-electron process) to improve the photocatalytic efficiency of H_2 production.

We report herein that water-soluble transition-metal complexes $[Rh^{III}(Cp^*)(bpy)(H_2O)](SO_4)$ (**1**; $Cp^* = \eta^5-C_5Me_5$, $bpy = 2,2'$ -bipyridine)^[16] and $[Ir^{III}(Cp^*)(H_2O)(bpm)Ru^{II}(bpy)_2](SO_4)_2$ (**2**; $bpm = 2,2'$ -bipyrimidine)^[17] act as efficient catalysts for photocatalytic hydrogen evolution in water at room temperature. The detailed kinetic analysis and detection of the intermediates, such as a one-electron-reduced complex, provide valuable insight into the mechanism of the photocatalytic hydrogen evolution, in which the

disproportionation of the one-electron-reduced complexes is the key step for the two-electron reduction of protons to H_2 .

Photocatalytic hydrogen evolution experiments were performed with $[Ru(bpy)_3]^{2+}$ ($2.0 \times 10^{-3} M$), a catalyst (**1**: $1.0 \times 10^{-3} M$, **2**: $1.0 \times 10^{-4} M$), ascorbic acid (H_2A , $0.8 M$), and sodium ascorbate ($NaHA$, $0.3 M$) at various pH values under irradiation with visible light ($\lambda > 430 nm$). No hydrogen evolution was detected in the absence of $[Ru(bpy)_3]^{2+}$ under otherwise identical experimental conditions. The formed hydrogen was identified and quantified by gas chromatography. The amount of evolved H_2 with **2** ($1.0 \times 10^{-4} M$) at pH 3.6 increased with irradiation time, and the turnover number (TON) per molecule of **2** reached 410 in 100 min (Figure S1 in the Supporting Information).

The quantum yield Φ of the photocatalytic hydrogen evolution was determined from the number of absorbed photons and the maximum hydrogen production rate using monochromatized light at $\lambda = 450 nm$ (see the Experimental Section). Under the present reaction conditions, in which the concentration of $[Ru(bpy)_3]^{2+}$ ($2.0 \times 10^{-3} M$) is 20 times larger than the concentration of **2** ($1.0 \times 10^{-4} M$), light is mainly absorbed by $[Ru(bpy)_3]^{2+}$ ($\lambda_{max} = 450 nm$, $\epsilon_{450nm} = 1.4 \times 10^4 M^{-1} cm^{-1}$) rather than **2** ($\lambda_{max} = 414 nm$, $575 nm$; $\epsilon_{450nm} = 5.2 \times 10^3 M^{-1} cm^{-1}$,^[17] see Figure S2 in the Supporting Information for the absorption spectra of $[Ru(bpy)_3]^{2+}$ and **2**). The pH dependence of Φ is shown in Figure 1, where the maximum Φ value (1.5×10^{-2}) is achieved at pH 3.6 for catalyst **2**.

The decrease of the Φ value when the pH value is decreased below 3.6 suggests that ascorbate ion (HA^-) rather than H_2A acts as an electron donor, because the pK_a value of H_2A is 4.0.^[18] The sharp decline in the Φ value when the pH value is increased above 3.6 may be explained by the formation of the low-valent iridium complex $[Ir^I(Cp^*)(H_2O)(bpm)Ru^{II}(bpy)_2]^{2+}$, which has no catalytic activity for hydrogen evolution, because the pK_a value of the iridium hydride complex derived from **2** ($[Ir^{III}(Cp^*)(H)(bpm)Ru^{II}(bpy)_2]^{3+}$) is 3.9.^[17] The lower Φ value at pH 3.6 for catalyst **1** (Figure 1) is consistent with the lower catalytic activity of **1** for H_2 evolution in the decomposition of formic acid.^[16,17] The decrease of the Φ value for complex **1** beyond pH 3.6 can be ascribed to the decrease of the concentration of protons, which react with the corresponding hydride $[Rh^{III}(Cp^*)(bpy)(H)]^+$. It should be noted that no H_2 was produced when **2** was replaced by $[Ir^{III}(Cp^*)(bpy)(H_2O)](SO_4)$ without the $\{Ru^{II}(bpy)_2\}$ unit, because the hydride complex $[Ir^{III}(Cp^*)(bpy)(H)]^+$ is stable at pH 3.6.^[19]

It is well known that the emission of the excited state of $[Ru(bpy)_3]^{2+}$ ($[Ru(bpy)_3]^{2+*}$) at $\lambda = 600 nm$ is efficiently

[*] Prof. Dr. S. Fukuzumi, T. Kobayashi, Dr. T. Suenobu
Department of Material and Life Science
Graduate School of Engineering, Osaka University
2-1 Yamada-oka, Suita, Osaka 565-0871 (Japan)
Fax: (+81) 6879-7370
E-mail: fukuzumi@chem.eng.osaka-u.ac.jp
Homepage: <http://www-etchem.mls.eng.osaka-u.ac.jp/>

Prof. Dr. S. Fukuzumi
Department of Bioinspired Science
Ewha Womans University, Seoul 120-750 (Korea)

[**] The support of two Grants-in-Aid (Nos. 20108010 and 21550061) and a Global COE program, "The Global Education and Research Center for Bio-Environmental Chemistry" from the Ministry of Education, Culture, Sports, Science, and Technology (Japan), and of KOSEF/MEST through WCU Project (R31-2008-000-10010-0) is gratefully acknowledged.

Supporting information for this article is available on the WWW under <http://dx.doi.org/10.1002/ange.201004876>.

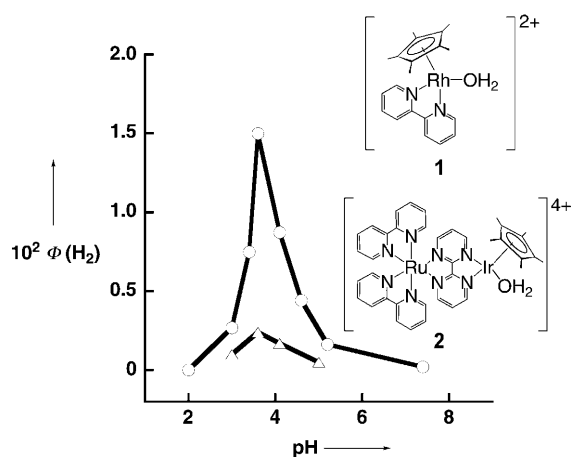


Figure 1. pH-dependence of the quantum yield (Φ) of photocatalytic H_2 evolution under irradiation of $[\text{Ru}(\text{bpy})_3]^{2+}$ ($2.0 \times 10^{-3} \text{ M}$) with monochromatized light ($\lambda = 450 \text{ nm}$) in a deaerated buffer solution containing **1** (Δ , $1.0 \times 10^{-4} \text{ M}$) or **2** (\circ , $1.0 \times 10^{-4} \text{ M}$) in the presence of $\text{H}_2\text{A}/\text{NaHA}$ (1.1 M) at various pH values at 298 K (light path length: 1 cm).

quenched in the presence of NaHA by photoinduced electron transfer from HA^- to $[\text{Ru}(\text{bpy})_3]^{2+*}$ (Figure S3 in the Supporting Information).^[20] The occurrence of the photoinduced electron transfer was confirmed by laser flash photolysis measurements. Nanosecond laser excitation at $\lambda = 455 \text{ nm}$ of a deaerated buffer solution containing $[\text{Ru}(\text{bpy})_3]^{2+}$, H_2A , and NaHA results in formation of $[\text{Ru}(\text{bpy})_3]^+$ (Figure 2). The transient absorption bands at $\lambda = 360$ and

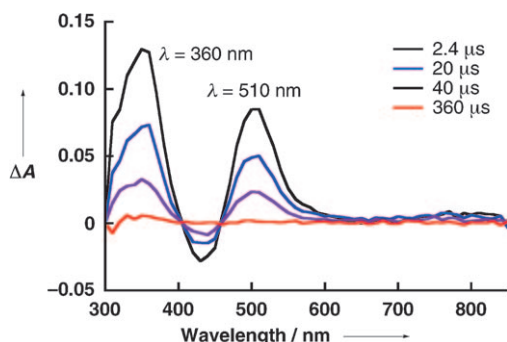


Figure 2. Transient absorption spectra after laser excitation of $[\text{Ru}(\text{bpy})_3]^{2+}$ ($8.0 \times 10^{-5} \text{ M}$) at $\lambda = 455 \text{ nm}$ in the presence of H_2A (0.8 M) and NaHA (0.3 M) in deaerated H_2O at pH 3.6 at 298 K.

510 nm are assigned to $[\text{Ru}(\text{bpy})_3]^+$.^[21] The absorption arising from ascorbate radical anion (A^-), which is produced by deprotonation of ascorbate radical (HA^\bullet),^[22] is overlapped at $\lambda = 360 \text{ nm}$. The decay of these transient absorption bands occurs by back electron transfer (BET) from $[\text{Ru}(\text{bpy})_3]^+$ to A^- to reproduce $[\text{Ru}(\text{bpy})_3]^{2+}$ and HA^- . The quantum yield of the generated $[\text{Ru}(\text{bpy})_3]^+$ in the presence of H_2A and NaHA was determined to be 10% using the comparative method (see the Supporting Information).^[23]

When **1** is added to the $[\text{Ru}(\text{bpy})_3]^{2+}/\text{H}_2\text{A}/\text{NaHA}$ system described in Figure 1, the same absorption bands ($\lambda_{\text{max}} = 350$

and 510 nm) arising from $[\text{Ru}(\text{bpy})_3]^+$ and A^- are observed 4 μs after laser excitation of a deaerated buffer solution at pH 3.6 containing $[\text{Ru}(\text{bpy})_3]^{2+}$, **1**, and $\text{H}_2\text{A}/\text{NaHA}$ (Figure 3a). However, the decay of the absorption bands at $\lambda = 350$ and 510 nm is accompanied by the appearance of an

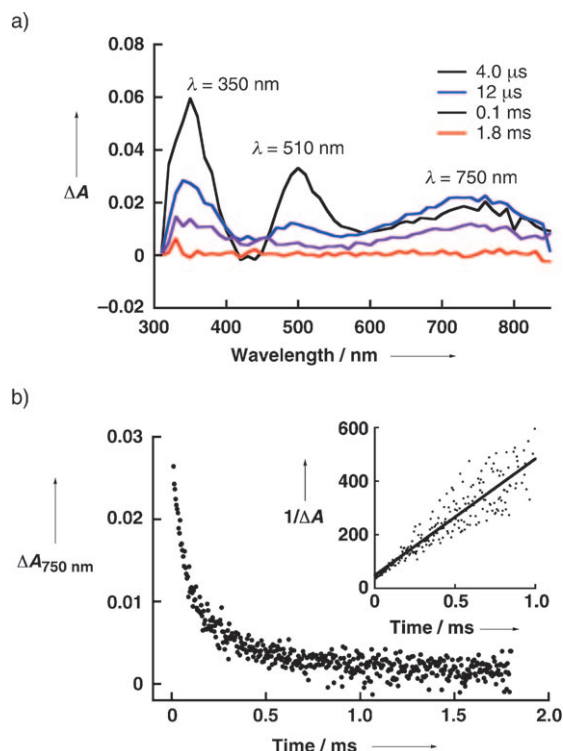


Figure 3. a) Transient absorption spectra after laser excitation of $[\text{Ru}(\text{bpy})_3]^{2+}$ ($8.0 \times 10^{-5} \text{ M}$) at $\lambda = 455 \text{ nm}$ in the presence of **1** ($1.6 \times 10^{-4} \text{ M}$), H_2A (0.8 M), and NaHA (0.3 M) in deaerated H_2O at pH 3.6 at 298 K. b) Decay time profile of the absorbance at $\lambda = 750 \text{ nm}$ arising from $[\text{Rh}^{\text{II}}(\text{Cp}^*)(\text{bpy})]^+$. Inset: Second-order plot.

absorption band at $\lambda = 750 \text{ nm}$. The newly formed absorption band at $\lambda = 750 \text{ nm}$ is assigned to the one-electron-reduced species of **1** ($[\text{Rh}^{\text{II}}(\text{Cp}^*)(\text{bpy})]^+$), because a similar absorption band has been reported for the Rh^{II} complex with a bipyridine derivative, $[\text{Rh}^{\text{II}}(\text{Cp}^*)(4,4'-(\text{COOH})_2\text{bpy})]^+$.^[15] This finding indicates that electron transfer from HA^- to the excited state ($[\text{Ru}(\text{bpy})_3]^{2+*}$) is followed by electron transfer from the resulting $[\text{Ru}(\text{bpy})_3]^+$ to **1** to produce the Rh^{II} complex.

The decay of transient absorption at $\lambda = 510 \text{ nm}$, assigned to $[\text{Ru}(\text{bpy})_3]^+$, obeys pseudo-first-order kinetics, and the pseudo-first-order rate constant increases linearly with concentration of **1** (Figure 4). The rate constant of electron transfer from $[\text{Ru}(\text{bpy})_3]^+$ to **1** was determined from the slope of the plot in Figure 4b to be $1.3 \times 10^9 \text{ M}^{-1} \text{ s}^{-1}$.

The decay of the transient absorption at $\lambda = 750 \text{ nm}$, assigned to $[\text{Rh}^{\text{II}}(\text{Cp}^*)(\text{bpy})(\text{H}_2\text{O})]^+$, at prolonged reaction time obeys second-order kinetics (Figure 3b) and does not obey first-order kinetics (Figure S4 in the Supporting Information). This result indicates that disproportionation of $[\text{Rh}^{\text{II}}(\text{Cp}^*)(\text{bpy})(\text{H}_2\text{O})]^+$ occurs to produce **1** and the Rh^{I} complex $[\text{Rh}^{\text{I}}(\text{Cp}^*)(\text{bpy})(\text{H}_2\text{O})]$.^[16] This resulting Rh^{I} com-

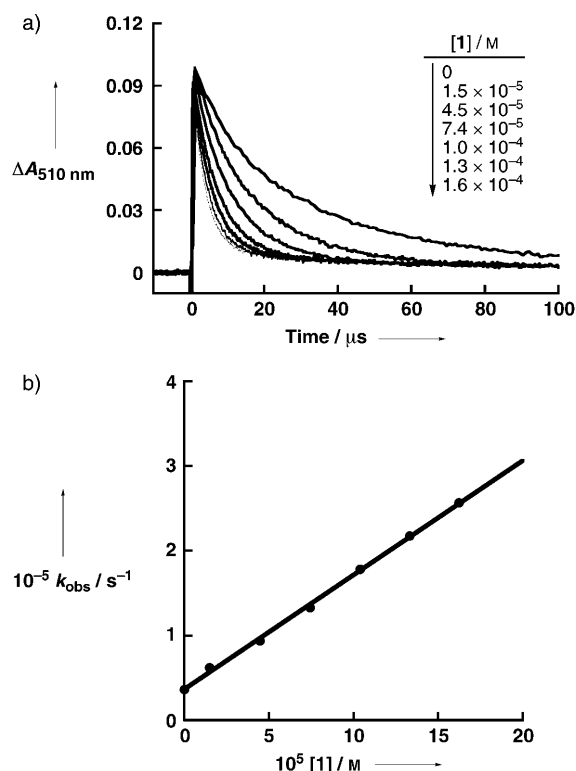


Figure 4. a) Decay time profiles at $\lambda = 510$ nm arising from $[\text{Ru}(\text{bpy})_3]^+$ in the presence of various concentrations of **1** in deaerated H_2O containing $[\text{Ru}(\text{bpy})_3]^{2+}$ ($8.0 \times 10^{-5} \text{ M}$), H_2A (0.8 M), and NaHA (0.3 M) at pH 3.6 at 298 K. b) Plot of the pseudo-first-order rate constant (k_{obs}) for electron transfer from $[\text{Ru}(\text{bpy})_3]^+$ to **1** versus $[\text{1}]$.

plex is immediately protonated at pH 3.6 to produce the rhodium hydride complex ($[\text{Rh}^{\text{III}}(\text{Cp}^*)(\text{H})(\text{bpy})]^+$), which reacts with a proton to generate H_2 , accompanied by regeneration of **1**.^[16]

Similar results were obtained for **2** by laser flash photolysis of a deaerated buffer solution at pH 3.6 containing $[\text{Ru}(\text{bpy})_3]^{2+}$, **2**, and $\text{H}_2\text{A}/\text{NaHA}$ (Figure 5). The rate constant of electron transfer from $[\text{Ru}(\text{bpy})_3]^+$ to **2** after electron transfer from HA^- to $[\text{Ru}(\text{bpy})_3]^{2+*}$ was determined to be $1.4 \times 10^9 \text{ M}^{-1} \text{ s}^{-1}$ (Figure S5 in the Supporting Information),

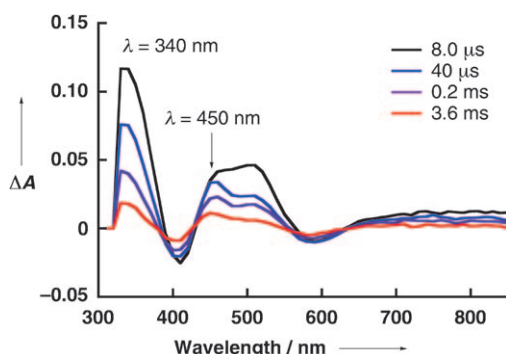
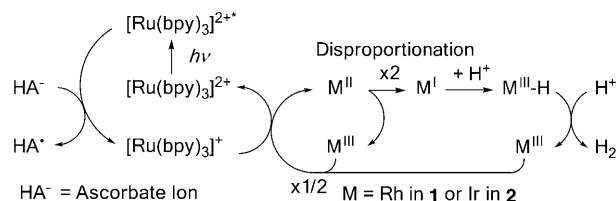


Figure 5. Transient absorption spectra after laser excitation of $[\text{Ru}(\text{bpy})_3]^{2+}$ ($8.0 \times 10^{-5} \text{ M}$) at $\lambda = 455$ nm in the presence of **2** ($8.9 \times 10^{-5} \text{ M}$), H_2A (0.8 M), and NaHA (0.3 M) in deaerated H_2O at pH 3.6 at 298 K.

which is virtually the same value as for **1**. The decay of the transient absorption at $\lambda = 450$ nm, assigned to $[\text{Ir}^{\text{II}}(\text{Cp}^*)(\text{H}_2\text{O})(\text{bpm})\text{Ru}^{\text{II}}(\text{bpy})_2]^{3+}$, obeys second-order kinetics (Figure S6 in the Supporting Information). The remaining absorption band, which extends into the NIR region, agrees with that of the Ir^{I} complex $[\text{Ir}^{\text{I}}(\text{Cp}^*)(\text{H}_2\text{O})(\text{bpm})\text{Ru}^{\text{II}}(\text{bpy})_2]^{2+}$.^[17] This finding clearly indicates that disproportionation of the Ir^{II} complex occurs to produce **2** and $[\text{Ir}^{\text{I}}(\text{Cp}^*)(\text{H}_2\text{O})(\text{bpm})\text{Ru}^{\text{II}}(\text{bpy})_2]^{2+}$. The Ir^{I} complex is protonated at pH 3.6 to produce the iridium hydride complex ($[\text{Ir}^{\text{III}}(\text{Cp}^*)(\text{H})(\text{bpm})\text{Ru}^{\text{II}}(\text{bpy})_2]^{3+}$), which reacts with a proton to generate H_2 , accompanied by regeneration of **2**.^[17]

Thus, the proposed mechanism of the photocatalytic generation of H_2 using HA^- , $[\text{Ru}(\text{bpy})_3]^{2+}$, and **1** or **2** is summarized in Scheme 1. The photoinduced electron transfer from HA^- to $[\text{Ru}(\text{bpy})_3]^{2+*}$ occurs to produce $[\text{Ru}(\text{bpy})_3]^+$,



Scheme 1. Photocatalytic generation of H_2 .

which reduces **1** and **2** to form $[\text{Rh}^{\text{II}}(\text{Cp}^*)(\text{bpy})(\text{H}_2\text{O})]^+$ and $[\text{Ir}^{\text{II}}(\text{Cp}^*)(\text{H}_2\text{O})(\text{bpm})\text{Ru}^{\text{II}}(\text{bpy})_2]^{3+}$, respectively. Disproportionation reactions of $[\text{Rh}^{\text{II}}(\text{Cp}^*)(\text{bpy})(\text{H}_2\text{O})]^+$ and $[\text{Ir}^{\text{II}}(\text{Cp}^*)(\text{H}_2\text{O})(\text{bpm})\text{Ru}^{\text{II}}(\text{bpy})_2]^{3+}$ proceed to produce $[\text{Rh}^{\text{I}}(\text{Cp}^*)(\text{bpy})(\text{H}_2\text{O})]$ and $[\text{Ir}^{\text{I}}(\text{Cp}^*)(\text{H}_2\text{O})(\text{bpm})\text{Ru}^{\text{II}}(\text{bpy})_2]^{2+}$, which are protonated to form the hydride complexes $[\text{Rh}^{\text{III}}(\text{Cp}^*)(\text{H})(\text{bpy})]^+$ and $[\text{Ir}^{\text{III}}(\text{Cp}^*)(\text{H})(\text{bpm})\text{Ru}^{\text{II}}(\text{bpy})_2]^{3+}$, respectively. Hydrogen is evolved in the reaction of the hydride complexes with a proton. No hydrogen evolution was detected upon irradiation of these hydride complexes when they were produced independently by reducing reagents such as formic acid or sodium borohydride.

In summary, photoinduced electron transfer from HA^- to $[\text{Ru}(\text{bpy})_3]^{2+*}$ (a one-electron process) leads to the two-electron reduction of protons to produce H_2 by disproportionation of the one-electron-reduced species of **1** and **2** to afford the two-electron-reduced metal complexes, which are protonated to give the metal hydride complexes. Hydrogen is produced by reactions of the metal hydride complexes with protons to regenerate **1** and **2**. Thus, disproportionation of the one-electron-reduced metal complexes has been demonstrated as the key step to enable the two-electron process (H_2 production) based on photoinduced electron transfer (a one-electron process).

Experimental Section

Compounds **1**, **2**, and $[\text{Ru}^{\text{II}}(\text{bpy})_2(\text{bpm})](\text{SO}_4)$ were synthesized according to literature procedures.^[16,17] All experiments were carried out under an Ar or N_2 atmosphere using standard Schlenk techniques

unless otherwise noted. Purification of water (18.2 MΩ cm) was performed with a Milli-Q system (Millipore; Direct-Q 3 UV).

The pH values of the solutions were determined by a pH meter (TOA, HM-20J) equipped with a pH combination electrode (TOA, GST-5725C). The pH value of the solution was adjusted using ascorbic acid (H₂A) and sodium ascorbate (NaHA).

An ascorbic acid buffer (H₂A/NaHA; 2.2 mmol, 2.0 mL) containing [Ru(bpy)₃]²⁺ (2.0 mM) and **1** or **2** (0.10 mM) was deaerated by freeze–pump–thaw cycles (three times) and flushed with nitrogen gas. The solution, contained in a quartz cuvette (light path length = 1 cm), was then irradiated with a xenon lamp (USHIO Optical Module X500) through a cut-off filter (Toshiba Y-43) transmitting λ > 430 nm at room temperature. The amount of evolved hydrogen gas was analyzed by a Shimadzu GC-14B gas chromatograph (N₂ carrier, active carbon with a particle size of 60–80 mesh at 353 K) equipped with a thermal conductivity detector.

The spectroscopic procedures and methods for quantum yield determination are described in the Supporting Information.

Received: August 5, 2010

Revised: October 5, 2010

Published online: December 22, 2010

Keywords: electron transfer · homogeneous catalysis · hydrogen · iridium · rhodium

- [1] N. S. Lewis, D. G. Nocera, *Proc. Natl. Acad. Sci. USA* **2006**, *103*, 15729–15735.
- [2] A. J. Esswein, D. G. Nocera, *Chem. Rev.* **2007**, *107*, 4022–4047.
- [3] J. T. Muckerman, E. Fujita, *ACS Symp. Ser.* **2009**, *1025*, 283–312.
- [4] S. Fukuzumi, *Eur. J. Inorg. Chem.* **2008**, 1351–1362.
- [5] M. Wang, Y. Na, M. Gorlov, L. Sun, *Dalton Trans.* **2009**, 6458–6467.
- [6] a) M. Kirch, J.-M. Lehn, J.-P. Sauvage, *Helv. Chim. Acta* **1979**, *62*, 1345–1384; b) M. Grätzel, *Acc. Chem. Res.* **1981**, *14*, 376–384.
- [7] a) S.-F. Chan, M. Chou, C. Creutz, T. Matsubara, N. Sutin, *J. Am. Chem. Soc.* **1981**, *103*, 369–379; b) C. V. Krishnan, B. S. Brunshwig, C. Creutz, N. Sutin, *J. Am. Chem. Soc.* **1985**, *107*, 2005–2015.
- [8] a) I. Okura, *Coord. Chem. Rev.* **1985**, *68*, 53–99; b) L. Persaud, A. J. Bard, A. Campion, M. A. Fox, T. E. Mallouk, S. E. Webber, J. M. White, *J. Am. Chem. Soc.* **1987**, *109*, 7309–7314.
- [9] a) E. D. Cline, S. E. Adamson, S. Bernhard, *Inorg. Chem.* **2008**, *47*, 10378–10388; b) F. Gärtner, B. Sundararaju, A.-E. Surkus, A. Boddien, B. Loges, H. Junge, P. H. Dixneuf, M. Beller, *Angew. Chem.* **2009**, *121*, 10147–10150; *Angew. Chem. Int. Ed.* **2009**, *48*, 9962–9965.
- [10] a) T. Lazarides, T. McCormick, P. Du, G. Luo, B. Lindley, R. Eisenberg, *J. Am. Chem. Soc.* **2009**, *131*, 9192–9194; b) P. Du, K. Knowles, R. Eisenberg, *J. Am. Chem. Soc.* **2008**, *130*, 12576–12577.
- [11] a) K. Sakai, H. Ozawa, *Coord. Chem. Rev.* **2007**, *251*, 2753–2766; b) R. Okazaki, S. Masaoka, K. Sakai, *Dalton Trans.* **2009**, 6127–6133.
- [12] a) H. Kotani, K. Ohkubo, Y. Takai, S. Fukuzumi, *J. Phys. Chem. B* **2006**, *110*, 24047–24053; b) H. Kotani, T. Ono, K. Ohkubo, S. Fukuzumi, *Phys. Chem. Chem. Phys.* **2007**, *9*, 1487–1492.
- [13] a) H. Ozawa, M. Haga, K. Sakai, *J. Am. Chem. Soc.* **2006**, *128*, 4926–4927; b) K. Yamauchi, S. Masaoka, K. Sakai, *J. Am. Chem. Soc.* **2009**, *131*, 8404–8406; c) Y. Miyake, K. Nakajima, K. Sasaki, R. Saito, H. Nakanishi, Y. Nishibayashi, *Organometallics* **2009**, *28*, 5240–5243.
- [14] a) S. Rau, B. Schäfer, D. Gleich, E. Anders, M. Rudolph, M. Friedrich, H. Görls, W. Henry, J. G. Vos, *Angew. Chem.* **2006**, *118*, 6361–6364; *Angew. Chem. Int. Ed.* **2006**, *45*, 6215–6218; b) M. Elvington, J. Brown, S. M. Arachchige, K. J. Brewer, *J. Am. Chem. Soc.* **2007**, *129*, 10644–10645; c) A. Fihri, V. Artero, M. Razavet, C. Baffert, W. Leibl, M. Fontecave, *Angew. Chem.* **2008**, *120*, 574–577; *Angew. Chem. Int. Ed.* **2008**, *47*, 564–567; d) H.-Y. Wang, W.-G. Wang, G. Si, F. Wang, C.-H. Tung, L.-Z. Wu, *Langmuir* **2010**, *26*, 9766–9771.
- [15] U. Kölle, M. Grätzel, *Angew. Chem.* **1987**, *99*, 572–574; *Angew. Chem. Int. Ed. Engl.* **1987**, *26*, 567–570.
- [16] S. Fukuzumi, T. Kobayashi, T. Suenobu, *ChemSusChem* **2008**, *1*, 827–834.
- [17] S. Fukuzumi, T. Kobayashi, T. Suenobu, *J. Am. Chem. Soc.* **2010**, *132*, 1496–1497.
- [18] E. G. Ball, *J. Biol. Chem.* **1937**, *118*, 219–239.
- [19] T. Abura, S. Ogo, Y. Watanabe, S. Fukuzumi, *J. Am. Chem. Soc.* **2003**, *125*, 4149–4154.
- [20] a) G. Neshvad, M. Z. Hoffman, *J. Phys. Chem.* **1989**, *93*, 2445–2452; b) L. A. Kelly, M. A. J. Rodgers, *J. Phys. Chem.* **1994**, *98*, 6377–6385.
- [21] Q. G. Mulazzani, S. Emmi, P. G. Fucchi, M. Z. Hoffman, M. Venturi, *J. Am. Chem. Soc.* **1978**, *100*, 981–983.
- [22] B. H. J. Bielski, D. A. Comstock, R. A. Bowen, *J. Am. Chem. Soc.* **1971**, *93*, 5624–5629.
- [23] K. Ohkubo, H. Kotani, J. Shao, Z. Ou, K. M. Kadish, G. Li, R. K. Pandey, M. Fujitsuka, O. Ito, H. Imahori, S. Fukuzumi, *Angew. Chem.* **2004**, *116*, 871–874; *Angew. Chem. Int. Ed.* **2004**, *43*, 853–856.